AMSI VACATIONRESEARCH SCHOLARSHIPS 2021–22

Get a taste for Research this Summer

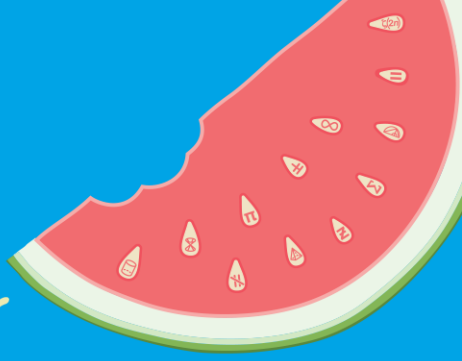

A Computational Approach to Population-Size-Dependent Branching Processes

Minyuan Li

Supervised by Dr. Sophie Hautphenne

The University of Melbourne

Vacation Research Scholarships are funded jointly by the Department of Education and the Australian Mathematical Sciences Institute.

AMSI AUSTRALIAN MATHEMATICAL SCIENCES INSTITUTE

Abstract

Matrix analytic methods are powerful tools to compute important performance measures of quasi-birth-and-death processes with finite level and phase spaces. In this report, we adapt these computational methods to two types of processes, called *total-progeny-dependent birth-and-death processes* and *population-size-dependent birth-and-death processes*, where the level and phase spaces are infinite in both cases. We use the adapted algorithms to compute several performance measures, including the total progeny size at extinction, the maximum population size and the mean extinction time for total-progeny-dependent birth-and-death processes, whereas we mainly focus on the feasible computational methods for the distribution of the total progeny size at extinction for population-size-dependent birth-and-death processes. Furthermore, we compare the distributions obtained from the algorithms to the empirical distributions obtained by simulation.

1 Introduction

Population-size-dependent branching processes (PSDBPs) form an important class of processes in the context of population evolution. The evolution of a species often depends on resources available in the environment, such as food and habitat, which are likely to be affected by the size of the population. Instead of assuming independence between individuals, PSDBPs provide more realistic models by allowing the evolutions of the population, such as the individual lifetime and reproduction rates, to be influenced by quantities that relate to its current population size. We wish to study these processes, and in particular, we are interested in *population-size-dependent birth-and-death processes*, where the birth and death rates of individuals depend on the current *population size*. Furthermore, we also focus on a new class of birth-and-death processes, called *total-progeny-dependent birth-and-death processes*, where the birth and death rates depend on the current *total progeny size*, that is, the cumulative number of children produced in the process until extinction of the population. This class of processes is designed to model the evolution of species with non-renewable resource consumption, or populations that consume resources at an extreme unsustainable manner, by assuming one-to-one correspondence between the available resources and the total progeny size (Hautphenne & Li 2022). We wish to study both types of processes in the context of *level-dependent quasi-birth-and-death processes*, which is a more general class of Markov processes equipped with analytic computational methods.

Level-dependent quasi-birth-and-death processes (QBDs) are two-dimensional structured Markov chains. The two dimensions are called the *level* and the *phase* of the process, and the generator of such process has a specific *tri-diagonal-block structure* (Latouche & Ramaswami 1999). QBDs form a rich class of processes, which can be used to model populations that evolve with different rules, and they are particularly useful when there exists an extra process or a variable that has an impact on the original process.

The corresponding algorithmic analytic methods, called the *matrix analytic methods*, which are generally developed for QBDs with *finite* level and phase spaces, are very powerful computational tools for performance measures of the processes. In particular, Hautphenne (2015) developed several explicit iterative algorithms to compute the distributions of key quantities of interest. The aim of this project is to adapt these existing numerical methods to *total-progeny-dependent birth-and-death processes* and *population-size-dependent birth-and-death processes*. The performance measures of interest include: the distribution of the total progeny size at extinction, the distribution of the maximum population size, and the mean extinction time.

The rest of the report is structured as follows. We introduce level-dependent quasi-birth-and-death processes and the corresponding matrix analytic methods in Section 2. Sections 3 and 4 discuss the adapted algorithms and compute some key performance measures of total-progeny-dependent birth-and-death processes and population-size-dependent birth-and-death processes. Finally, Section 5 draws a conclusion and provides the potential future work directions.

Statement of authorship

Sophie Hautphenne provided the supervision and the main directions of the project, as well as the previous work on the algorithms adapted in this project. Minyuan Li adapted and modified the algorithms, produced the results with computations in MATLAB, and wrote this report.

2 Algorithmic computations for level-dependent quasi-birth-and-death processes (QBDs)

Quasi-birth-and-death processes form a broader and more general class of Markov processes compared to the class of birth-and-death processes. We first introduce this rich class of processes, and then focus on the matrix analytic methods, which are the computational methods for performance measures tailored for this class of processes.

2.1 Level-dependent quasi-birth-and-death processes (QBDs)

A *level-dependent quasi-birth-and-death process* $\{X(t), \varphi(t)\}$ is a two-dimensional continuous-time Markov chain, where $X(t)$ and $\varphi(t)$ are called the *level* and the *phase* at time t, respectively. We denote the level space as N and phase space as $L(k)$, which depends on the level k. At each transition, the level is only allowed to move up by one, down by one, or stay the same. This gives the generator of such processes a very specific tri-diagonal-block structure (Latouche & Ramaswami 1999):

$$Q = \begin{bmatrix} A_0^{(0)} & A_1^{(0)} & 0 & 0 & \cdots \\ A_{-1}^{(1)} & A_0^{(1)} & A_1^{(1)} & 0 & \cdots \\ 0 & A_{-1}^{(2)} & A_0^{(2)} & A_1^{(2)} & \cdots \\ 0 & 0 & A_{-1}^{(3)} & A_0^{(3)} & \ddots \\ \vdots & \vdots & \vdots & \ddots & \ddots \end{bmatrix}, \tag{1}$$

where the block matrix $A_i^{(k)}, i = -1, 0, 1$ contains the transition rates from (k, p_1) to $(k+i, p_2)$, for $p_1 \in L(k)$ and $p_2 \in L(k+i)$. If all entries in $A_0^{(0)}$ and $A_1^{(0)}$ are 0's, then the process has an absorbing level at 0. We define *extinction* as the event that the process is absorbed at level 0.

2.2 Matrix analytic methods

Matrix analytic methods use the specific tri-diagonal structure of the generator to compute performance measures for QBDs. The algorithms outlined in Hautphenne (2015) aim to compute quantities such as the

extinction probability, the maximum population size, and the expected time until extinction. However, these algorithms only consider the QBDs *with finite level and phase spaces*. In this project, we aim to modify and apply these algorithms to other types of continuous-time Markov processes. We now introduce the definition of a few quantities used in our reference paper, which will also be referred to in the rest of the report.

2.2.1 The matrices $G_k(M)$

The sequence of matrices $G_k(M), 1 \leq k \leq M$, is used for computing the extinction probability and the maximum population size, where $(G_k(M))_{ij}$ denotes the probability of the process reaching level $k-1$ before going over level M, and the phase at that time is j, given that the process starts at level k, in phase i. That is,

$$(G_k(M))_{ij} = \mathbb{P}[\gamma(k-1) < \gamma(M+1), \varphi(\gamma(k-1)) = j \mid X(0) = k, \varphi(0) = i], \quad 1 \leq k \leq M, \tag{2}$$

where $\gamma(k)$ denotes the first hitting time in level k.

In particular, we are interested in $G_1(M)$, which contains the probabilities of the QBD reaching level 0 without going over level M, provided that it starts in level 1. The cap M provides the convenience to start from $G_M(M)$ and iterate forward to compute $G_1(M)$ (Hautphenne 2015). We can remove this restriction by taking M to infinity.

For QBDs that go extinct with probability one, the matrices $G_1(m), m = 1, 2, \ldots$ can be used to compute the distribution of the maximum population size. Specifically, the probability that the maximum population size of such processes is m is equal to the difference between the first row sums of the matrices $G_1(m)$ and $G_1(m-1)$, that is,

$$\mathbf{p}(m) = (G_1(m) - G_1(m-1)) \cdot \mathbf{1}, \tag{3}$$

where $\mathbf{1}$ is a column vector of 1's, with its length matching the size of $G_1(m)$. The i^{th} entry in the vector $\mathbf{p}(m)$ represents the conditional probability given the process starts with one individual in phase i.

2.2.2 The vectors $\mathbf{d}_k^{(M)}$

The sequence of vectors $\mathbf{d}_k^{(M)}, 1 \leq k \leq M$, is used for computing the expected time until absorption at level 0, that is, the expected time until extinction for the QBDs. Consider a QBD truncated at level $M+1$, and set level 0 and level $M+1$ both to be absorbing levels. The i^{th} entry in the vector $\mathbf{d}_k^{(M)}$ represents the expected time of such a truncated process to hit level $k-1$ on the paths where it will be absorbed at level 0 before reaching level $M+1$, given that the process starts at level k, in phase i:

$$(\mathbf{d}_k^{(M)})_i = \mathbb{E}[\gamma(k-1)\mathbb{1}_{\gamma(0)<\gamma(M+1)} \mid X(0) = k, \varphi(0) = i]. \tag{4}$$

Note that as M increases to infinity, the sequence of the vectors $\mathbf{d}_1^{(M)}$ converges to the expected extinction times for the process starting with one individual.

The details of the algorithms to compute the performance measures of the QBDs are outlined in Hautphenne (2015), and now we move on to adapt the methods to other processes.

3 Total-progeny-dependent birth-and-death processes

Total-progeny-dependent birth-and-death processes $\{Z(t), X(t)\}$ form a specific class of QBDs, where the level $Z(t)$ and the phase $X(t)$ represent the population size and the total progeny size at time t, respectively. At each transition, the process is only allowed to have either one birth event, $(z, x) \to (z+1, x+1)$, or a death event, $(z, x) \to (z-1, x)$. The individual birth rate $b(x)$ and death rate $d(x)$ are dependent on the current phase x, that is, on the cumulative number of children produced in the population up to the current point.

One of the difficulties to apply the matrix analytic methods directly is that the level and phase spaces of the QBDs where the algorithms apply are finite, whilst in total-progeny-dependent birth-and-death processes, the spaces of population and total progeny size are infinite. In order to address this issue, we truncate the spaces with reference to the deterministic approximations of the mean maximum population size and the mean total progeny size at extinction in Hautphenne & Li (2022) to get some idea about the truncation points. Moreover, we take a step further to provide more information on the quantities of interest than the results shown in Hautphenne & Li (2022), as the numerical algorithms are known to converge to the full correct distributions. The model we consider here is: $b(x) = \frac{\lambda}{x}, d(x) = \mu$, where $b(x)$ and $d(x)$ represent individual birth rate and death rate respectively, and μ is taken to be 1 for simplicity.

3.1 Total progeny size distribution at extinction

To investigate the total progeny size distribution at extinction, we first compute the matrix $G_1(M)$, where $(G_1(M))_{1j}$ represents the probability that the process goes extinct before reaching population size $M+1$, and the total progeny at extinction is j, given that there is one individual and the total progeny size is one when the process starts. As $M \to \infty$, the first row of $G_1(M)$ converges to the distribution of the total progeny size at extinction. After applying the appropriate truncation, we can compute this quantity by directly applying the iterative approach in Hautphenne (2015).

In Figure 1, we compare the total progeny size distribution with the mean value obtained from its deterministic approximation from Hautphenne & Li (2022), and with a normal distribution whose mean and variance are the conditional mean and variance from the total progeny size distribution, conditioning on having at least one birth event before the process goes extinct. It appears that, as we increase λ, the distribution of the total progeny size at extinction, given that there is at least one birth event, approaches the normal distribution. Furthermore, as λ increases, the conditional mean of the total progeny becomes the mean value from the deterministic approximation.

One of the possible reasons that the conditional distribution of the total progeny size at extinction converges to the normal distribution is due to diffusion, which is out of scope of this project.

3.2 Maximum population size

As total-progeny-dependent birth-and-death processes go extinct with probability one, based on the idea introduced in Section 2.2.1 and because the initial phase is 1, starting with one individual at time 0, the

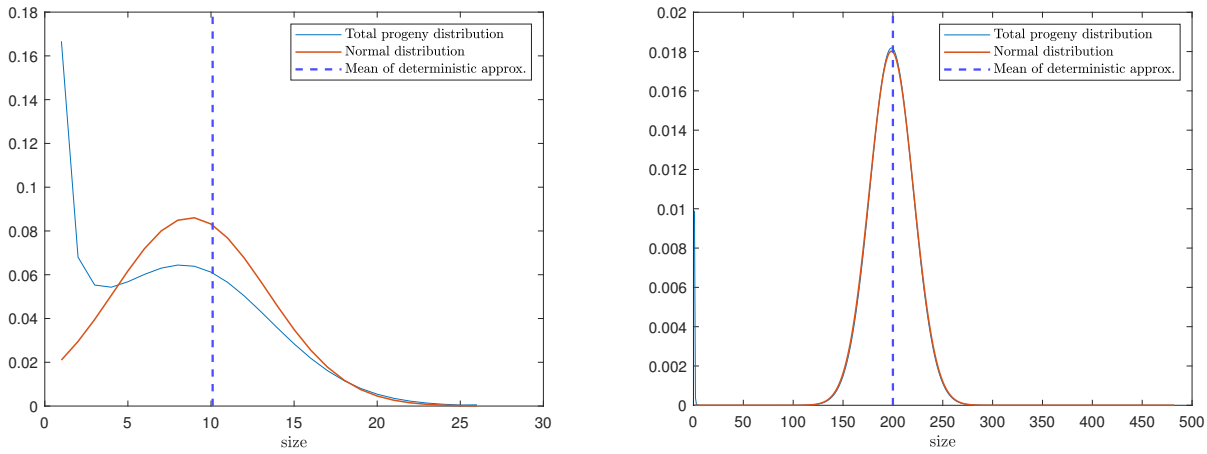

Figure 1: **Total progeny distribution at extinction** — Left: $\lambda = 5$; Right: $\lambda = 100$.

probability of the maximum population size being m is

$$p(m) = \mathbf{e}_1 \cdot G_1(m) \cdot \mathbf{1} - \mathbf{e}_1 \cdot G_1(m-1) \cdot \mathbf{1}, \tag{5}$$

where $\mathbf{e}_1$ is a row vector that matches the size of $G_1(m)$, with the first entry to be 1 and 0 for the rest. Using a similar approach as in the case of the distribution of the total progeny size at extinction, in Figure 2, we compare the maximum population distribution obtained from the algorithm to the normal distribution with mean and variance equal to the conditional mean and conditional variance of the maximum population distribution (conditional on at least one birth event happening). Furthermore, we add the maximum population we would obtain from the deterministic approximation in Hautphenne & Li (2022) to both plots. From this figure, we can see that, similar to the distribution of the total progeny size at extinction, as we increase the value of λ, the distribution we obtained from the algorithm exhibits more normality. However, in this case, the maximum population size from the deterministic approximation is below the mean of the distribution from the algorithm in both plots. This result can also be visually seen in Hautphenne & Li (2022), but with the increase of λ, the relative size of the underestimation will decrease and converge to zero.

3.3 Mean extinction time

The iterative algorithm described in Hautphenne (2015) to compute the mean time until extinction can be adapted to the total-progeny-dependent case, with the modified truncated matrices as in previous sections. In Figure 3, we compare the mean time to extinction obtained from the algorithm to the corresponding mean from 50000 simulations. We can see that the result from the algorithm corresponds well with the simulations.

In contrast to the issue of estimating the mean extinction time in Hautphenne & Li (2022) where the deterministic approximation does not give a direct estimate of the quantity of interest, the algorithm we adapted here gives a much more accurate estimate. However, as the algorithm involves iterative computation, when we increase the value of λ, the algorithm suffers from computational efficiency.

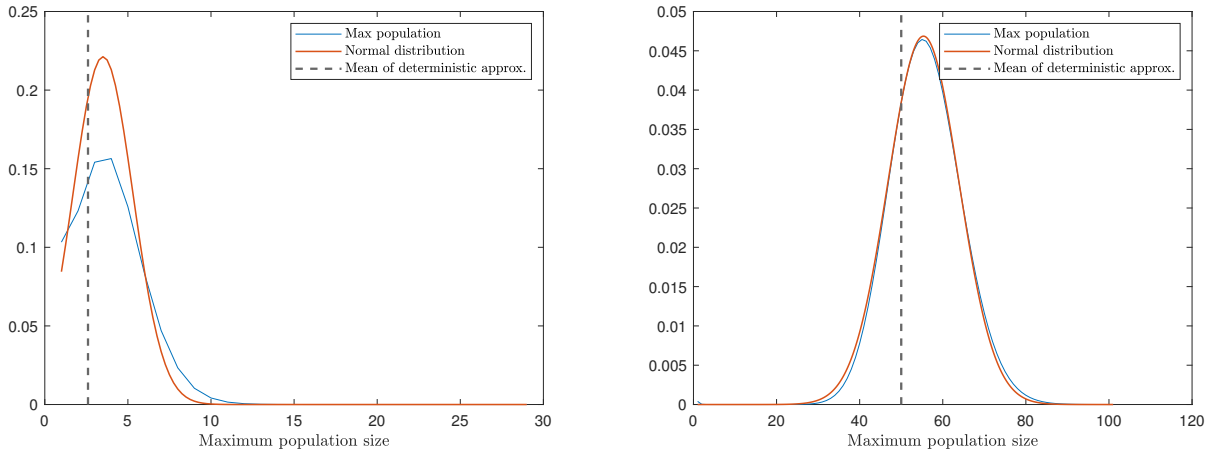

Figure 2: **Total progeny distribution at extinction** — Left: $\lambda = 5$; Right: $\lambda = 100$.

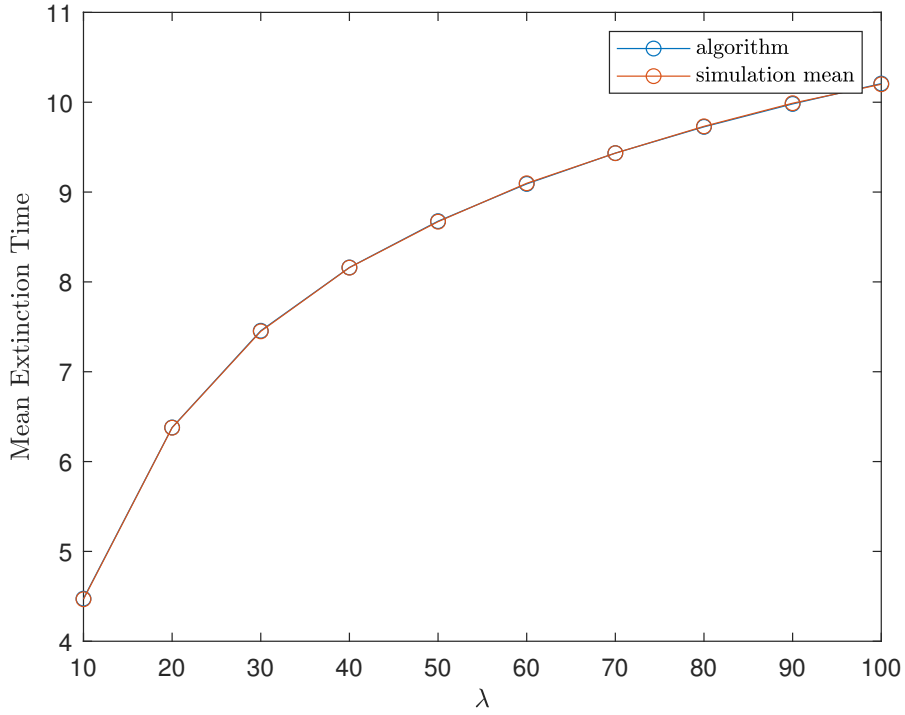

Figure 3: **Mean extinction time vs λ**

4 Population-size-dependent birth-and-death-processes

A population-size-dependent birth-and-death process $(X(t))_{t\geq 0}$ is a one dimensional continuous-time Markov process, where $X(t)$ is the population size at time t. As in any birth-and-death processes, at each transition, the population size can only go up by one or down by one. However, different from total-progeny-dependent birth-and-death processes, the birth and death rates in a population-size-dependent birth-and-death process

depend on the current population size the process is at (not the total progeny size). A typical trajectory of such processes is shown in Figure 4. It lingers around its carrying capacity K, the population size where the birth rate is equal to the death rate, for a long time before it goes extinct eventually with probability one.

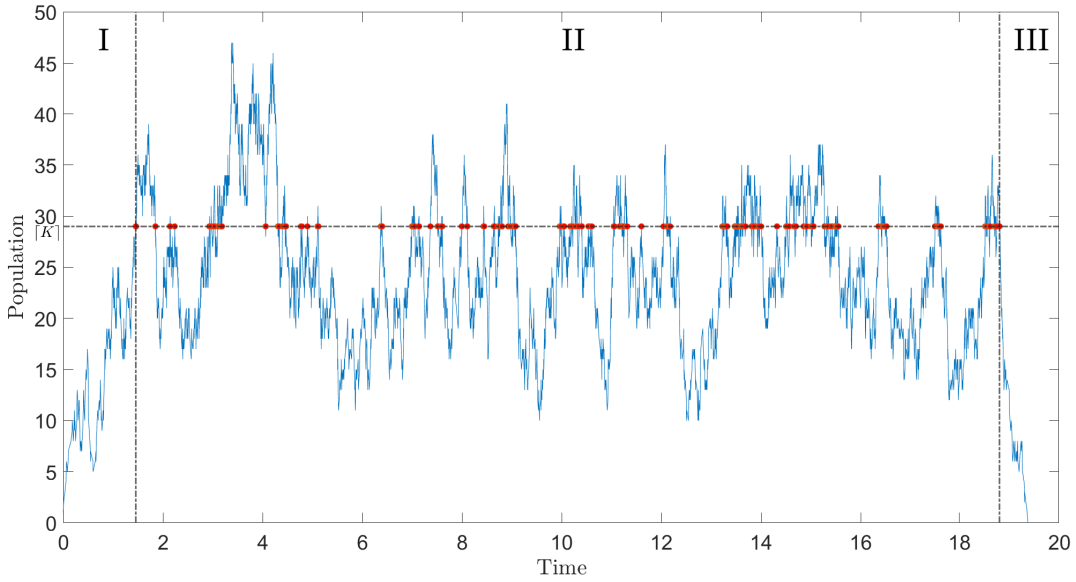

Figure 4: **A typical trajectory of population-size-dependent BDP,** $K = 29$**.**

4.1 Total progeny size distribution at extinction

As we are interested in studying the total progeny size distribution at extinction, we add the total progeny size as another dimension to the original process to make it a QBD. Therefore, the population-size-dependent birth-and-death process we are considering is a two-dimensional process $\{X(t), \varphi(t)\}_{t\geq 0}$, where $X(t)$ and $\varphi(t)$ represent the population level and the total progeny size at time t respectively. The spaces of both dimensions are from 1 to infinity.

Unlike the situation in the previous sections, the notion of carrying capacity in population-size-dependent birth-and-death processes creates difficulty in directly applying the algorithm. As mentioned previously, we need finite level and phase spaces to apply the algorithms. However, as the population lingers around the carrying capacity for a long time, the total progeny size at extinction is likely to be very large even for a small K. Therefore, it is very difficult to find a reasonable point to truncate the phase space, and the huge size of the phase space leads to computational inefficiency and numerical instability in matrix inversions and multiplications.

In order to address this issue, we consider two cases: processes that go extinct before population reaches level K, and processes whose population reaches level K before going extinct. We assume without loss of generality that K is an integer.

For the first case, the population space is bounded at K, and we can truncate the total progeny space at a relatively small multiple of K to apply the algorithm as before. In this case, the distribution of the total

progeny size at extinction, $\varphi(\gamma(0))$, given that the population will not reach level K, follows the first row of $(G_1(K-1))$ normalized by its sum.

For the second case, we further partition the trajectories of the process into three parts: the initial part where its population starts with one individual and reaches K for the first time, the middle part where its population reaches K for the first time and returns to K for the last time, and the last part where its population starts from K and reaches 0 without going back to K. We denote the cumulative number of progeny in each section as U, V and W, respectively. Figure 4 visually highlights the three parts, and we discuss how we obtain the distributions of U, V, and W in the next three subsections.

4.2 Part 1: Reaching K for the first time

We are interested in the conditional distribution of the cumulative progeny size during the interval of time between the start of the process with one individual and the time it reaches K individuals for the first time, given that the process reaches K before getting extinct. This can be computed by using the methods in Hautphenne (2015). First we consider the matrix $F_1(M)$, where the $(i,j)^{th}$ entry represents the probability that the population of the process reaches level $M+1$ before going extinct, and the total progeny size at the time of reaching $M+1$ is j, given that the process starts with population size one and total progeny size i, that is,

$$F_1(M) = \mathbb{P}[\gamma(M+1) < \gamma(0), \varphi(\gamma(M+1)) \mid X(0) = 1, \varphi(0)], \quad M \geq 1. \tag{6}$$

In our case, we want to obtain the first row of matrix $F_1(K-1)$. Using the Markov property, the matrix $F_1(K-1)$ can be decomposed into a product of matrices $L_1 L_2 \cdots L_{K-1}$, where matrix L_i contains the probabilities of the process reaching population level $i+1$ before going extinct, given that the process starts with i individuals. That is,

$$L_i = \mathbb{P}[\gamma(i+1) < \gamma(0), \varphi(\gamma(i+1)) \mid X(0) = i, \varphi(0)], \quad i \geq 1. \tag{7}$$

Using Proposition 3.3 in Hautphenne (2015), the sequence of matrices L_i's can be computed by first-step analysis in an iterative manner.

Recall that U is defined to be the cumulative progeny size until the population reaches K for the first time, given that it starts from population size one and reaches K before going extinct. Note that the probability mass function of U is recorded in the row vector $\mathbf{e_1} \cdot F_1(K-1)/(\mathbf{e_1} \cdot F_1(K-1) \cdot \mathbf{1})$.

Figure 5 shows the distribution of U obtained from both simulations and the algorithm. The left panel confirms that the distribution computed by the algorithm corresponds very well with the empirical distribution obtained from the simulations. The right panel shows that as the carrying capacity increases, the mode of the distribution shifts to the right.

It is also worth noting that with the same technique, we can compute and compare the distribution of the progeny size at different proportions of the carrying capacity. Figure 6 plots the distribution of the cumulative progeny size centred around the mode at $0.55K, 0.6K, 0.95K$ and K, given that the process reaches each respective level, with $K = 52$ on the left panel and $K = 351$ on the right panel. Visually in both panels, it can be seen that roughly all distributions have a similar shape which is skewed to the right.

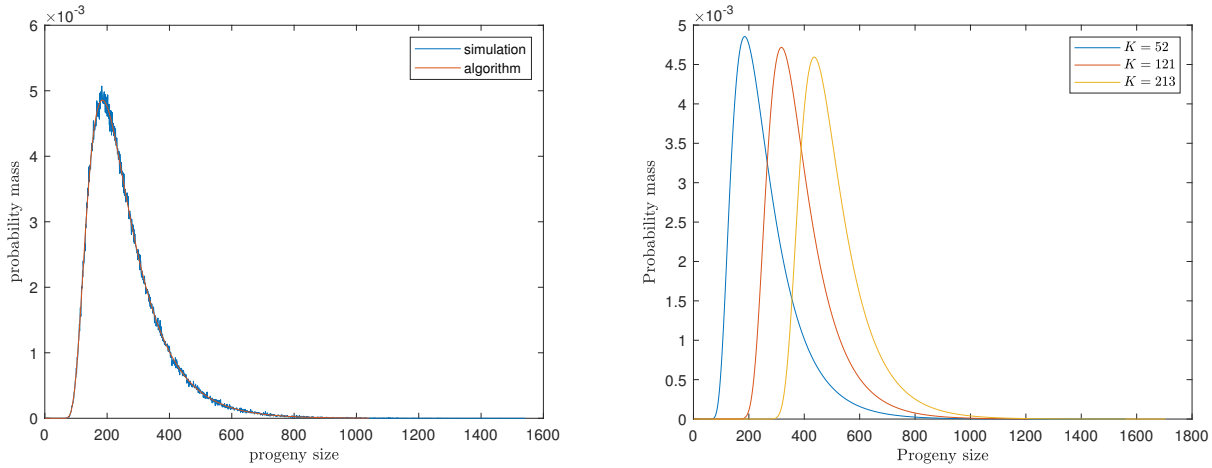

Figure 5: **Progeny size distribution until reaching K for the first time** — Left: Conditional distributions from 10^6 simulations and the algorithm, $K = 52$; Right: Conditional distributions from the algorithm, with $K = 52, 121, 213$.

However, the distributions at $0.55K$ and $0.6K$ clearly have smaller dispersions compared to the ones at $0.95K$ and K. Furthermore, the distributions at $0.55K$ and $0.6K$ are more similar to each other compared to the ones at $0.95K$ and K. This becomes more visually obvious with larger carrying capacities in the right panel. It may suggest that there is more stochastic randomness when the process gets closer to the carrying capacity. As the population increases between one and K, the difference between the birth and death rates decreases, which reduces the pull towards the carrying capacity. Also note that comparing each distribution in the left panel with those in the right panel, it appears that the increase in the carrying capacity reduces the variance in each distribution. This is because the larger the population size, the more deterministic the trajectories, therefore the smaller the variability.

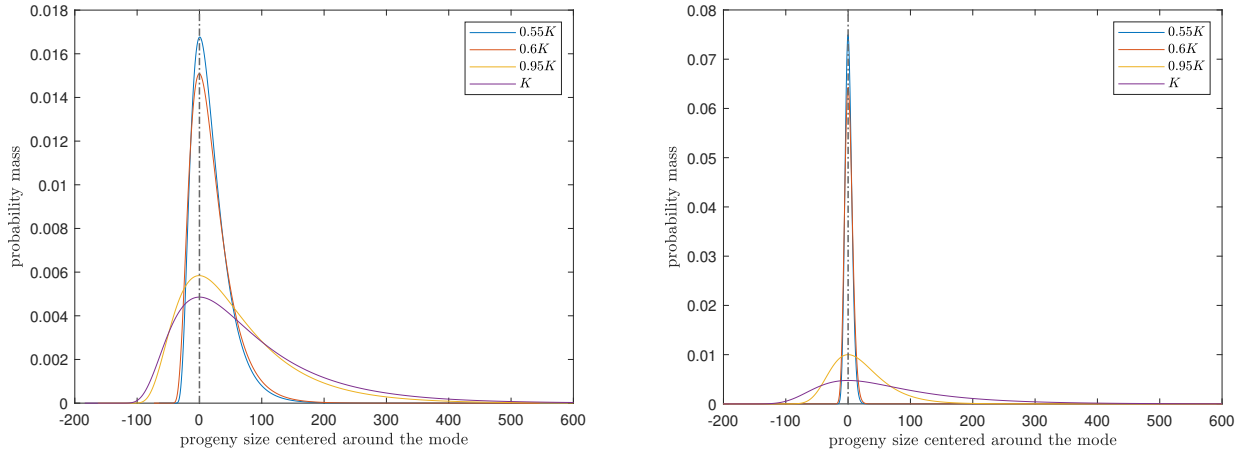

Figure 6: **Distribution of progeny size centred around the mode** — Left: $K = 52$; Right: $K = 351$.

4.3 Part 2: The transient renewal process between first and last visits at K

The time that a typical trajectory of a population-size-dependent birth-and-death process lingers around the carrying capacity has the order (at most) e^{cK} for some constant $c > 0$, and note that this is an asymptotic result for large K (Hamza et al. 2016). It suggests that (even with a small carrying capacity) the cumulative progeny size at the last visit of K, given that the process starts at K, can be very large. Therefore, it is computationally infeasible to directly use the truncated QBD approach to compute its distribution.

Therefore, instead of trying to directly compute the distribution of the cumulative progeny size over the entire lingering part, we first consider the number of times the population returns to K, given that it starts at K, before it starts its final descent to extinction. We denote this quantity by N, and note that N takes non-negative integer values, including zero. By the Markov property, each time the population reaches K, it should have the same probability to return to K before going extinct, independent of the number of times it has already returned to K. That is, N follows a Geometric distribution with parameter $1 - f_K$, where f_K denotes the probability the population returns to K before going extinct, given that it starts at K, that is,

$$f_K = \mathbb{P}[\gamma^+(K) < \gamma(0) \mid X(0) = K], \tag{8}$$

where $\gamma^+(K)$ denotes the first return time for the population to level K, given it starts from K.

We claim that:

$$f_K = 1 - \frac{d(K)}{b(K) + d(K)} \mathbf{e}_1 \cdot \left(\prod_{i=1}^{K-1} G_i(K-1) \right) \cdot \mathbf{1}. \tag{9}$$

Indeed, to compute f_K, we consider its complement, the probability that the population reaches 0 without returning to K, given that it starts at level K. For the complement event to happen, the population must move down one level for the first step. Next, recall the definition of $G_i(M)$, which contains the probabilities of reaching population level $i-1$ without going over level M, given that it starts at level i. Therefore, the product of such matrices for $i = 1$ to $K-1$ gives the probabilities we desire. The k^{th} entry in the first row of the product represents the probability $\mathbb{P}[\gamma^+(K) < \gamma(0), \varphi(\gamma^+(K)) = k-1 \mid X(0) = K, \varphi(0) = 0], \quad k = 1, 2, \ldots$. Note that in this case, $\mathbf{e}_1$ corresponds to starting in phase 0, therefore the expression in (9) follows.

Let the random variables Y_i, $i = 1, 2, \ldots$ denote the count of the cumulative progeny size produced between the i^{th} and the $(i+1)^{st}$ visits to the carrying capacity (given that there is a $(i+1)^{st}$ visit to K), that is,

$$\mathbb{P}(Y_i = y) = \mathbb{P}[\varphi(\gamma_{i+1}(K)) = y + j \mid \varphi(\gamma_i(K)) = j, \gamma_{i+1}(K) < \infty], \quad \forall j = 1, 2, \ldots, \tag{10}$$

where $\gamma_i(K)$ denotes the i^{th} time the population reaches K.

By the Markov property, Y_i's form a sequence of random variables that are independent and identically distributed. Therefore, we only need to focus on the distribution of an arbitrary Y_i, and we can write V, the cumulative progeny size in the interval between the times where the population reaches level K for the first time and the last time, as $V = \sum_{i=1}^{N} Y_i$. As the population lingers around K, the size of Y_i tends to be relatively small, therefore it is easier to truncate both the population space and the cumulative progeny size space to apply the algorithms.

To compute the distribution of Y_i, we first truncate the population space and the total progeny space at M and T (respectively), and it suffices to let M and T be small multiples of K. Then we define the matrix

$$G^{(K)}(M) = \mathbb{P}[\gamma^+(K) < \min(\gamma(0), \gamma(M+1)), \varphi(\gamma^+(K)) \mid X(0) = K, \varphi(0)]. \tag{11}$$

Note that $\mathbf{e}_1 \cdot G^{(K)}(M) = \mathbb{P}[\gamma^+(K) < \min(\gamma(0), \gamma(M+1)), \varphi(\gamma^+(K)) \mid X(0) = K, \varphi(0) = 0]$ gives (an approximation of) the distribution of Y_i, and $\mathbf{e}_1 \cdot G^{(K)}(M) \cdot \mathbf{1}$ gives an approximation of f_K, for large values of M and T. Furthermore, we claim

$$\begin{aligned} G^K(M) = (-A_0^{(K)})^{-1} A_1^{(K)} G_{K+1}(M) \\ + (-A_0^{(K)})^{-1} A_{-1}^{(K)} \mathbb{P}[\gamma(0) > \gamma(K), \varphi(\gamma(K)) \mid X(0) = K-1, \varphi(0)]. \end{aligned} \tag{12}$$

When the population takes the first step going one unit up, we need to compute the probabilities of the population returning to K without going over the truncated level M, given that the population starts at K. This is exactly the definition of $G_{K+1}(M)$, and we can apply the algorithm to compute this matrix. When the population takes the first step going one unit down, the probability matrix we need to compute is explicitly expressed. Indeed, to compute the second matrix in (12), if we relabel the states in such a way that for any state i between 0 and K, $i \to K-i$, then we would obtain a related QBD process $\{X'(t), \varphi'(t)\}$. The generator of the new related process has the same structure as the original process, and $A_0'^{(k)} = A_0^{(K-k)}$, $A_{-1}'^{(k)} = A_1^{(K-k)}$ and $A_1'^{(k)} = A_{-1}^{(K-k)}$. This type of processes are also introduced in Latouche & Ramaswami (1999), where they are referred to as *level-reversed processes*. Therefore,

$$\mathbb{P}[\gamma(0) > \gamma(K), \varphi(\gamma(K)) \mid X(0) = K-1, \varphi(0)] = G_1'(K-1), \tag{13}$$

where $G_1'(K-1)$ denotes the matrix $G_1(K-1)$ for the process $\{X'(t), \varphi'(t)\}$. Any algorithm to compute $G_1'(K-1)$ can then be used to obtain the matrix $G^{(K)}(M)$.

The left panel of Figure 7 compares the distribution of Y_i obtained from the algorithm and the simulations. The two curves overlay each other very well, suggesting that the method using the algorithm is appropriate. We can also observe from the distribution that the probability masses decrease quickly as the progeny size increases, but with a long tail to the right. Furthermore, the right panel plots the distributions of Y_i for different values of K, and we can see that the distributions are very similar even though the values of K vary significantly. However, different values of K do have a significant impact on f_K, which will impact the final distribution of the total progeny size at extinction.

4.4 Part 3: From the last visit at K to extinction

Finally, we look into the distribution of W, the cumulative progeny size produced between the last visit to K and absorption at level 0. As the population will not go over level K, we can truncate the population space at K. Similar to the case in Part 1, we can also truncate the cumulative progeny size at a relatively small multiple of K.

Next, we define the probability matrix

$$F_{K-1}(K) = \mathbb{P}[\gamma(0) < \gamma(K), \varphi(\gamma(0)) \mid X(0) = K-1, \varphi(0)], \tag{14}$$

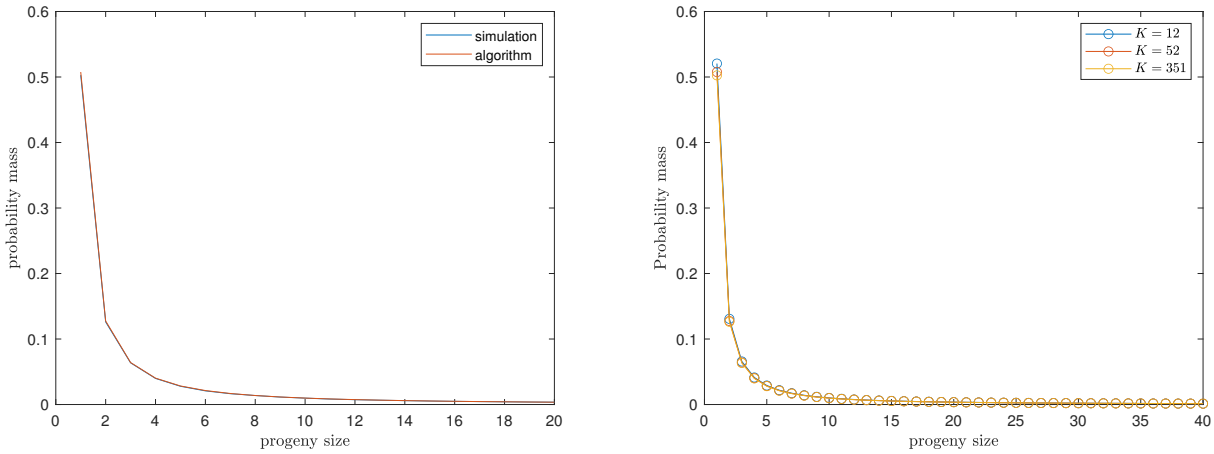

Figure 7: **Distribution of Y_i** — Left: By simulation and algorithm, $K = 52$; Right: Distributions from the algorithms for different Ks.

Similar to the case in Section 4.3, $\mathbf{e}_1 \cdot (F_{K-1}(K))/(\mathbf{e}_1 \cdot (F_{K-1}(K)) \cdot \mathbf{1})$ gives the distribution of W.

Again, using similar ideas of conditioning on each downward step and the Markov property, we have:

$$F_{K-1}(K) = \prod_{K-1 \geq i \geq 1} G_i(K-1). \tag{15}$$

Figure 8 compares the distribution of W obtained from the algorithm to the empirical distribution obtained from simulations. One of the difficulties in such comparison is that we need to simulate the entire trajectory of the process to produce one realisation for the population to go from the last K to 0, which is very inefficient. Nevertheless, we can still see that the algorithm result roughly matches the empirical distribution.

4.5 Final distribution

Now we are ready to combine the previous sections to come up with the distribution of $\varphi(\gamma(0))$, the total progeny size at extinction. At the start of the process, the population will reach the carrying capacity with probability $\mathbf{e}_1 \cdot F_1(K-1) \cdot \mathbf{1}$, and it will go extinct before reaching the carrying capacity with the complement probability. Therefore, $\varphi(\gamma(0))$ follows a mixture distribution:

$$\varphi(\gamma(0)) \sim \begin{cases} \mathbf{e}_1 \cdot G_1(K-1)/(\mathbf{e}_1 \cdot G_1(K-1) \cdot \mathbf{1}) & \text{w.p. } \mathbf{e}_1 \cdot F_1(K-1) \cdot \mathbf{1}, \\ U + V + W & \text{w.p. } 1 - \mathbf{e}_1 \cdot F_1(K-1) \cdot \mathbf{1}. \end{cases} \tag{16}$$

In the case where the population reaches K before going extinct, we can use its probability generating function to explicitly write out the distribution for small values of carrying capacity K. Note that the random variables U, Y_i, N and W are all mutually independent and $V = \sum_{i=1}^{N} Y_i$, therefore using the probability generating function, we have:

$$G_{\varphi(\gamma(0))|\{\gamma(K)<\gamma(0)\}}(s) = G_U(s) G_N(G_{Y_i}(s)) G_W(s), \tag{17}$$

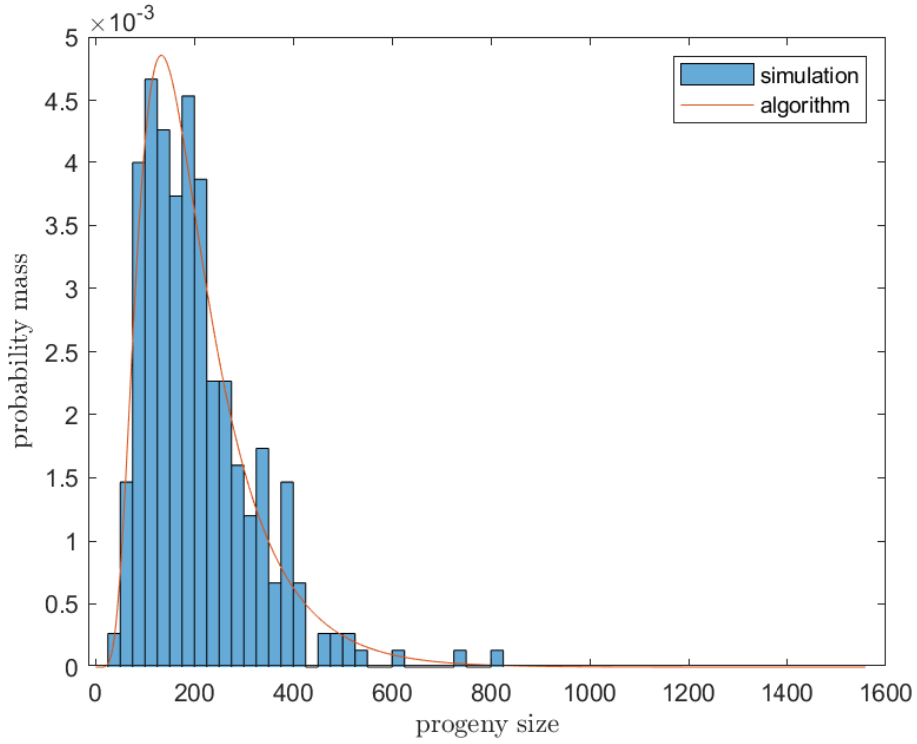

Figure 8: **Distribution of W obtained by 300 simulations and by the algorithm,** $K = 52$.

where $G_\cdot(s)$ is the probability generating function with respect to the respective random variables. We can then use the numerical methods in Abate & Whitt (1992) to insert the probability generating function of $\varphi(\gamma(0))$. However, this method is feasible only with small K, as the size of the total progeny increases quickly with the increase in K. The left panel in Figure 9 shows this distribution with $K = 16$.

With larger values of K, we can empirically construct the distribution by simulating the random variables U, V, and W and take their sum to obtain a realisation of the total progeny size at extinction, given that the process reaches the carrying capacity before going extinct. This provides a feasible and efficient way to empirically visualise the distribution, as opposed to simulating the entire trajectories, which is computationally infeasible with large carrying capacities. The right panel of Figure 9 shows the distribution obtained by 50000 simulations with $K = 52$.

5 Discussion and Conclusion

We started our discussion on a general class of Markov processes called level-dependent quasi-birth-and-death processes, and introduced the matrix analytic methods that are designed to compute performance measures of QBDs with finite level and phase spaces. We then focused on total-progeny-dependent birth-and-death processes, where we adapted the QBD algorithms by truncating the population and the total progeny spaces with reference to the deterministic approximations in Hautphenne & Li (2022). For population-size-dependent birth-and-death processes, we investigated the distribution of the total progeny size at extinction

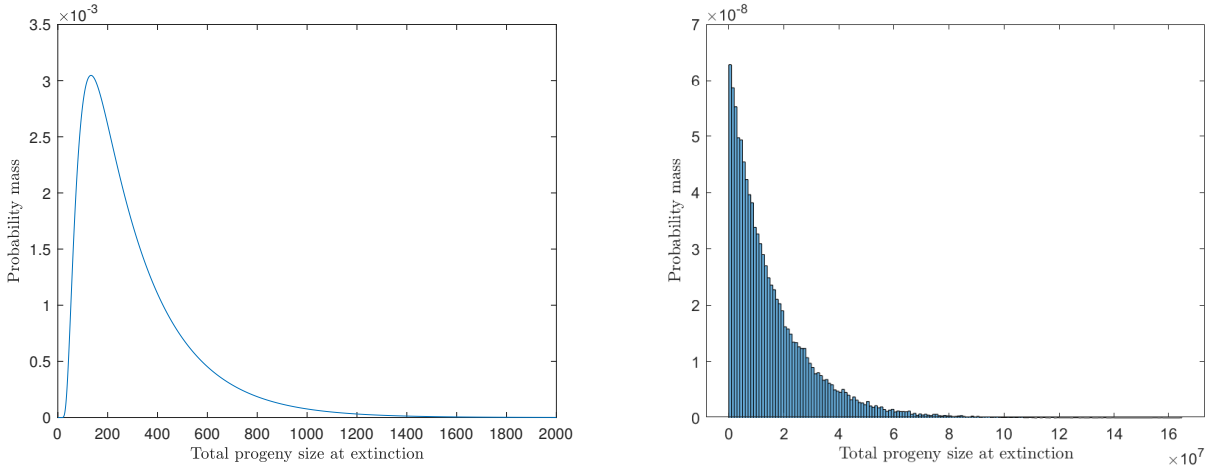

Figure 9: **Distribution of the total progeny size at extinction given the carrying capacity is reached** — Left: by probability generating function, $K = 16$; Right: by 50000 simulations, $K = 52$.

by partitioning the process into three parts, given that the process reaches the carrying capacity before going extinct, and adapted the algorithms in each part to obtain the result we desire.

From our discussions throughout the report, we can conclude that the algorithms we adapted provide us with means to compute important performance measures with computational efficiency and accuracy for the two processes we are interested in. This allows us to further understand and explore the behaviour of these processes.

However, it is also worth pointing out that the matrix analytic methods we adapted rely on the tri-diagonal-block structure of the generator. Therefore, these algorithms do not work on other more complex processes, such as population-size-dependent birth-and-death processes with catastrophe events, where the generator exhibits a lower-triangular-block structure with an extra upper diagonal. As one of our future directions, we can attempt to develop other computational techniques that would allow us to understand the evolution of such processes, with further reference in Latouche et al. (1984).

6 Acknowledgements

Minyuan Li would like to acknowledge the AMSI for the research opportunity and Dr. Sophie Hautphenne for the valuable advice and constant support throughout the project.

References

Abate, J. & Whitt, W. (1992), 'Numerical inversion of probability generating functions', *Operations Research Letters* **12**(4), 245–251.

Hamza, K., Jagers, P. & Klebaner, F. C. (2016), 'On the establishment, persistence, and inevitable extinction of populations', *Journal of Mathematical Biology* **72**(4), 797–820.

Hautphenne, S. (2015), 'A structured Markov chain approach to branching processes', *Stochastic Models* **31**(3), 403–432.

Hautphenne, S. & Li, M. (2022), 'A fluid approach to total-progeny-dependent birth-and-death processes', *to appear in Stochastic Models* .

Latouche, G., Jacobs, P. & Gaver, D. (1984), 'Finite Markov chain models skip-free in one direction', *Naval Research Logistics Quarterly* **31**(4), 571–588.

Latouche, G. & Ramaswami, V. (1999), *Introduction to matrix analytic methods in stochastic modeling*, SIAM.